



Development and validation of a prognostic model and gene co-expression networks for breast carcinoma based on scRNA-seq and bulk-seq data

Zhaohui Ruan^{1#}, Dongmei Chi^{2#}, Qianyu Wang¹, Jiabin Jiang¹, Qi Quan¹, Jinxin Bei³, Roujun Peng¹

¹VIP Section Department, State Key Laboratory of Oncology in South China, Sun Yat-sen University Cancer Center, Guangzhou, China;

²Department of Anesthesiology, State Key Laboratory of Oncology in South China, Sun Yat-sen University Cancer Center, Guangzhou, China;

³Department of Experimental Research, State Key Laboratory of Oncology in South China, Sun Yat-sen University Cancer Center, Guangzhou, China

Contributions: (I) Conception and design: Z Ruan, R Peng; (II) Administrative support: None; (III) Provision of study materials or patients: Z Ruan, D Chi; (IV) Collection and assembly of data: Z Ruan, D Chi, Q Wang; (V) Data analysis and interpretation: Z Ruan, D Chi, Q Wang; (VI) Manuscript writing: All authors; (VII) Final approval of manuscript: All authors.

[#]These authors contributed equally to this work.

Correspondence to: Prof. Roujun Peng, VIP Section Department, State Key Laboratory of Oncology in South China, Sun Yat-sen University Cancer Center, Dongfeng East Road, Guangzhou 510060, China. Email: pengrj@sysucc.org.cn.

Background: Breast carcinoma is the most common malignancy among women worldwide. It is characterized by a complex tumor microenvironment (TME), in which there is an intricate combination of different types of cells, which can cause confusion when screening tumor-cell-related signatures or constructing a gene co-expression network. The recent emergence of single-cell RNA sequencing (scRNA-seq) is an effective method for studying the changing omics of cells in complex TMEs.

Methods: The Dysregulated genes of malignant epithelial cells was screened by performing a comprehensive analysis of the public scRNA-seq data of 58 samples. Co-expression and Gene Set Enrichment Analysis (GSEA) analysis were performed based on scRNA-seq data of malignant cells to illustrate the potential function of these dysregulated genes. Iterative LASSO-Cox was used to perform a second-round screening among these dysregulated genes for constructing risk group. Finally, a breast cancer prognosis prediction model was constructed based on risk grouping and other clinical characteristics.

Results: Our results indicated a transcriptional signature of 1,262 genes for malignant breast cancer epithelial cells. To estimate the function of these genes in breast cancer, we also constructed a co-expression network of these dysregulated genes at single-cell resolution, and further validated the results using more than 300 published transcriptomics datasets and 31 Clustered Regularly Interspaced Short Palindromic Repeats (CRISPR) screening datasets. Moreover, we developed a reliable predictive model based on the scRNA-seq and bulk-seq datasets.

Conclusions: Our findings provide insights into the transcriptomics and gene co-expression networks during breast carcinoma progression and suggest potential candidate biomarkers and therapeutic targets for the treatment of breast carcinoma. Our results are available via a web app (<https://prognosticpredictor.shinyapps.io/GCNBC/>).

Keywords: Breast cancer; single-cell RNA sequencing; gene co-expression networks; prognostic model; iterative least absolute shrinkage and selection operator (LASSO)

Submitted Oct 31, 2022. Accepted for publication Dec 07, 2022.

doi: 10.21037/atm-22-5684

View this article at: <https://dx.doi.org/10.21037/atm-22-5684>

Introduction

Breast carcinoma arises from the epithelial cells of the breast and is the most common malignant tumor in women worldwide. A recent study estimated there were about 2.3 million new cases of breast cancer each year globally (1). Various treatment strategies that target specific molecular subtypes of breast carcinoma, such as progesterone receptor-positive (PR+) cells and human epidermal growth factor receptor 2-positive (HER2+) cells, have greatly improved the survival outcomes for about 70–80% of breast cancer patients (2), suggesting that the identification of additional molecular subtypes may also provide better survival in these patients. However, further research is needed to identify prognosis-related biomarkers and the functions and molecular mechanisms of these molecules.

The tumor, node, metastasis staging system of malignant tumors (TNM stage) is universally recognized as a significant predictor of clinical outcomes. However, its predictive power is limited, and increasing evidence suggests that the prognosis of breast cancer patients is not only related to the TNM stage but also the expression levels of key biomarkers. In particular, previous transcriptional analyses that used bulk RNA-seq data found that changes in the levels of *SMC4*, *UBE2C*, and *JAM2* mRNAs were related to breast cancer prognosis (3–5). Given the

heterogeneous composition of the tumor microenvironment (TME), which includes T cells, B cells, and numerous other cell types, coupled with the fact that many different types of cells can affect breast carcinoma progression (6–8), the use of bulk RNA-seq to identify dysregulated genes in breast cancer may generate misleading results. Moreover, analysis of the co-expression networks in breast cancer using bulk RNA-seq, an approach widely used to describe gene interactions and molecular mechanisms, could also produce misleading results.

Bulk RNA-sequencing (Bulk RNA-seq) is the method that detects transcriptomics profiles of biopsies. It shows the average expression of genes across numerous cells (9).

On the other hand, single-cell transcriptional sequencing (scRNA-seq) is a transcriptome technology that can simultaneously quantify gene expression at the genome-wide level in thousands of individual cells (10,11) and provides a solution to help address the above-mentioned issues (screening of tumor-cell-related biomarkers and construction of gene co-expression networks). Thus, scRNA-seq is a powerful tool for studying heterogeneous tissues, such as the TME. More specifically, scRNA-seq can reduce the false-positive identification of differentially expressed genes (DEGs) that may be caused by multiple non-target cell types in the TME, and is well-suited for determining the differences between tumor and normal cells. This new method also facilitates the study of gene-gene relationships, thus enabling the investigation of co-expression networks (12). Several recent scRNA-seq studies have examined the heterogeneous environment of breast carcinoma (11,13), with a particular focus on the tumor immune microenvironment and cancer cell subpopulations. These scRNA-seq datasets are a useful resource for researchers attempting to identify novel breast cancer molecular subtypes and improve prognostic prediction. However, few studies have focused on the transcriptomic signature of malignant epithelial cells in breast carcinoma, especially their gene co-expression network. Moreover, today, most breast cancer treatments are primarily directed against tumor cells. We believe that a prognostic model for tumor cells can better guide treatment strategy. Therefore, we built a prognostic model based on genes that focus on tumor cells screened from scRNA-seq data. This approach has been utilized to study other tumors (14–16); however, breast cancer has not yet been examined.

In this work, we used publicly available breast cancer scRNA-seq data to compare the transcriptomic changes in breast malignant epithelial cells to those of non-

Highlight box

Key findings

- Constructed gene co-expression networks based on scRNA-seq data of malignant epithelial cells of breast cancer.
- Constructed a well-performed malignant cell-related prognostic model for breast cancer.
- Established a web app for other researchers to get our results.

What is known and what is new?

- There were lots of studies about constructing gene co-expression networks and prognostic models based on bulk RNA-seq which may be noised by the gene expression of other components of the tumor microenvironment.
- Here, we constructed gene co-expression networks and a well performed prognostic model based on scRNA-seq data of malignant cells of breast cancer and evaluated them in multiple data.

What is the implication, and what should change now?

- Our results provide insights into the mechanisms underlying breast carcinoma progression and suggest potential therapeutic strategies for the treatment of this cancer.

malignant epithelial cells and obtained a set of 1,262 genes that are dysregulated in malignant breast epithelial cells. To examine the functions of these dysregulated genes, we constructed co-expression networks for all 1,262 genes in individual malignant epithelial cells using scRNA-seq data and performed pathway enrichment analysis to annotate their functions. We then utilized over 300 published transcriptomics datasets and 31 Clustered Regularly Interspaced Short Palindromic Repeats (CRISPR) screening data to verify the co-expression networks. On this basis, iterative least absolute shrinkage and selection operator (LASSO) Cox analysis was used to conduct the second round of screening, and a collection of breast cancer prognosis-related gene sets consisting of 10 genes was obtained; thus, a new breast cancer patient prognostic stratification strategy was constructed. Finally, we constructed a breast cancer prognostic prediction model with good predictive power based on risk grouping and other clinical characteristics. Our model performed well in both internal cohort and external cohort. Our analyses of malignant breast epithelial cells will provide a characterization of the transcriptomic mechanisms and gene co-expression networks during the progression of breast carcinoma, and may also help identify novel biomarkers and therapeutic targets. We present the following article in accordance with the TRIPOD reporting checklist (available at <https://atm.amegroups.com/article/view/10.21037/atm-22-5684/rc>).

Methods

Single-cell data retrieval and processing

The scRNA-seq data in this study were obtained from Gene Expression Omnibus (GEO: GSE161529) (17) and included data from *in situ* breast carcinoma and control samples (such as adjacent tissues from breast cancer patients and normal breast tissue from patients without breast cancer). Samples from precancerous lesions and lymph nodes were excluded. Scrublet (<https://github.com/swolock/scrublet>) was used to predict doublets in these data using an expected doublet rate of 0.06 and default parameters otherwise (18). The SoupX R package (<https://github.com/constantAmateur/SoupX>) was employed to estimate and remove cell-free mRNA contamination in the droplets (19). The study was conducted in accordance with the Declaration of Helsinki (as revised in 2013).

Further quality control was then applied using key metrics, including the number of unique genes detected

in each cell ($n_{\text{Feature_RNA}} > 500$), the total number of detected molecules ($n_{\text{Count_RNA}} > 1,000$), and the percentage of mitochondrial genes in each cell ($\text{percent.mt} < 25\%$). Seurat's pipeline (<https://github.com/satijalab/seurat/>) was used for dimensional reduction and unsupervised clustering after quality control (20). The specific steps were as follows: (I) normalization of the data using the `NormalizeData` and `ScaleData` functions of the Seurat package (20); (II) selection of 3,000 hypervariable genes for downstream analysis using the `FindVariableFeatures` function; and (III) calculation of 30 principal components for dimensionality reduction. Since each sample was processed separately, "batch effect" was a possibility. Thus, Harmony (<https://github.com/immunogenomics/harmony>) was used to correct for the batch effect between patients (21). `RunUMAP` and the `FindClusters` function were used to reduce dimensionality and identify clusters ($\text{dims} = 1:30$, $\text{resolution} = 0.3$). Finally, epithelial cells were identified using universal markers.

Identification of malignant epithelial cells and DEGs

The evidence for somatic alterations of large-scale chromosomal copy number variants (gains or losses) in single cells was determined using `inferCNV` with the default parameters (<https://github.com/broadinstitute/inferCNV>). To distinguish malignant and non-malignant cells in the tumor sample-derived epithelial cells, we performed the following analysis. First, epithelial cells from the standard control samples were annotated a reference. Second, the clustering algorithm was applied to all of the epithelial cells from tumor samples. Third, a second round of dimensional reduction and unsupervised clustering was performed to identify epithelial cell subsets. Finally, cell clusters with high chromosome copy number variations (CNVs) relative to the control (reference) were considered malignant. To be specific, clusters with higher CNVs was defined as malignant epithelial cells. On the contrast, clusters with lower CNVs was defined as malignant epithelial cells

Next, we analyzed the differential expression in malignant epithelium relative to the non-malignant epithelium using the `FindMarkers` function from the Seurat package. Genes were considered to be differentially expressed based on the standard thresholds ($\text{avg_log_FC} > 0.25$ or $\text{avg_log_FC} < -0.25$, adjusted $P < 0.05$). Only genes that had higher expression in malignant cells ($\text{avg_log_FC} > 0.25$, adjusted $P < 0.05$) were considered to be DEGs and

subjected to further co-expression gene analysis.

Co-expression of DEGs

To assess gene co-expression, Spearman's rank correlation coefficient was determined for all possible combinations of DEGs, and the Benjamini-Hochberg method was used to correct these P values for multiple comparisons. Thus, for each DEG gene i , any other gene whose expression exhibited a significant correlation (adjusted $P < 0.05$) was defined as a co-expressed gene.

Functional enrichment of DEGs

The method of Li *et al.* (22) was employed for the functional annotation of the DEGs. Briefly, for gene j and another gene i , the rank score (RS) was calculated using the adjusted P value ($adjP_{ij}$), and the correlation coefficient (R_{ij}) was calculated as follows:

$$RS = -\log_{10} adjP_{ij} \times \text{sgn}(R_{ij}) \quad [1]$$

Next, all genes were sorted according to the RS and were used in a pre-ranked gene set enrichment analysis (GSEA) to identify potentially related pathways. The fgsea package (<https://github.com/ctlab/fgsea>) was used for GSEA analysis (23), with a focus on the Hallmark gene sets, which were downloaded from the Sigdb database (<https://www.gsea-msigdb.org/gsea/msigdb/>). Gene sets with an adjusted P value lower than 0.05 in the GSEA were defined as correlated pathways (24).

Validation of the gene co-expression networks and functional enrichment of the DEGs

The Search-Based Exploration of Expression Compendium (SEEK: <https://seek.princeton.edu/seek/>) was utilized to validate the gene co-expression networks (25). For the co-expression network of each gene, the top 100 co-expressed genes (due to the input limits of SEEK) with the highest RS values were screened for verification. Only data sets related to breast carcinoma were used for validation. The data sets with P values (provided by SEEK) below 0.05 were considered suitable for co-expression verification.

CRISPR screening data were downloaded from The Biological General Repository for Interaction Datasets (BioGRID) (<https://orcs.thebiogrid.org/>) (26). The datasets related to breast carcinoma and cell proliferation were used for verification. For each dataset, genes related to

cell proliferation were defined according to their original author's choice. Briefly, a gene whose Hit value was "yes"1 was considered to be related to cell proliferation. Genes that included cell proliferation-related pathways (E2F targets, G2M checkpoint, MYC targets V1, MYC targets V2, P53 pathway, and mitotic spindle; adjusted P value < 0.05 and NES > 0 ; screened only in genes that are highly expressed in malignant cells) in their co-expression gene pathway enrichment results were also considered to be related to cell proliferation (27).

Construction of a DEG-based COX prognostic model

Data collection

TGCA-BRCA cohort (internal cohort) bulk RNA-seq data for breast carcinoma were downloaded from the UCSC Xena (<http://xena.ucsc.edu/>) (28). All of the analyzed tissue samples were from patients who had primary breast carcinoma and were older than 18 years of age. Patients with unknown race, age, TNM stage, or gender were excluded. A standard data collection and filtering workflow was used (Figure 1A). The external cohort data (METABRIC cohort) was downloaded from cBioportal (<https://www.cbioportal.org/>).

Risk group construction

DEGs from the single-cell RNAseq data were used to construct a breast cancer-related risk group. First, the bulk RNA-seq data for breast carcinoma patients [from The Cancer Genome Atlas (TCGA)] were divided into a training set (60%) and a testing set (40%). In the training set, the iterative LASSO technique was used to screen for characteristic genes in the model. The workflow for risk group construction utilized defined procedures (Figure 1B). Initially, 3,000 iterations were used for variable screening of the DEGs from the scRNA-seq analysis using a LASSO-penalized multivariate Cox proportional hazards model with the three-fold cross-validation set (29). Next, genes in the DEGs were sorted according to their frequency in the 3,000 iterations, and genes with the highest frequency were considered an important signature for the prediction of patient survival. Subsequently, the 10 most frequent genes were selected to construct a risk score with Cox regression. The following equation was applied to calculate the risk score, in which the coefficients were from the Cox regression:

$$\text{Risk score} = \sum_{i=1}^n \text{coefficient}_i \times \text{gene}_i \quad [2]$$

Thereafter, the Variance Inflation Factor (VIF) was

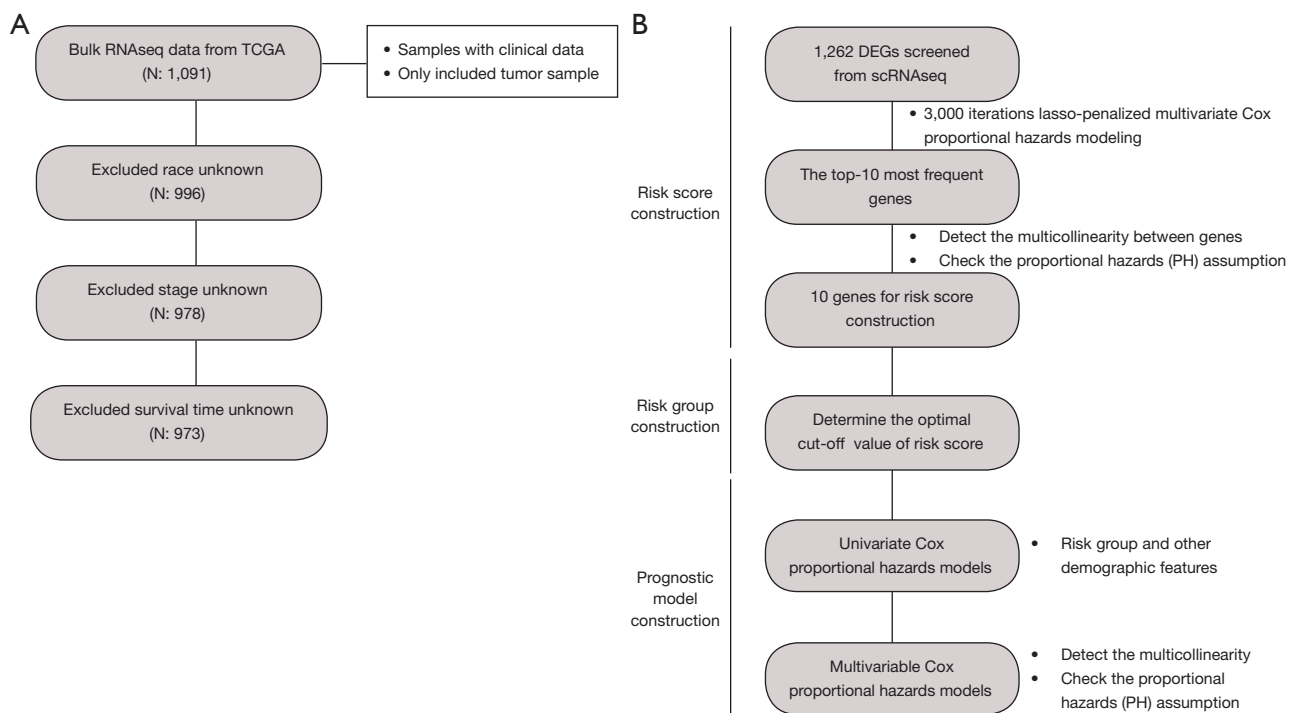


Figure 1 Workflow of the data selection and the construction of the prognostic model. (A) Workflow used for data selection in the prognostic model construction. (B) Workflow used to determine risk score, risk group, and construction of the prognostic model. TCGA, The Cancer Genome Atlas; DEG, differentially expressed gene.

used to assess collinearity between genes (threshold: $VIF = 4$) (30). The `cox.zph` function was employed to check the proportional hazards (PH) assumption (31), and features with P values greater than 0.05 were considered to satisfy the PH assumption. Lastly, receiver operating characteristic (ROC) analysis was performed used to determine the model accuracy and the optimal cut-off value for patient stratification.

Construction and evaluation of the COX prognostic model

We constructed a prognostic model to predict overall survival in breast cancer patients. Univariable Cox regression analysis was performed to screen for prognostic factors and clinical factors (age, gender, stage, race, and risk group). All variables with P values less than 0.05 in the univariable Cox regression analysis were included in the multivariate Cox regression analysis. Collinearity was determined based on the VIF, and the PH assumption of variables in the multivariate Cox regression analysis was confirmed. The area under the curve (AUC) was used to assess the prognostic value of the model at different times

in the internal (TCGA cohort) and external (METABRIC cohort) cohorts.

Differences between DEGs in the scRNA-seq and bulk RNA-seq data

The bulk RNA-seq data for breast carcinoma were downloaded from UCSC Xena (<http://xena.ucsc.edu/>) (28). Tissue samples from carcinomas *in situ* and normal tissues were retained for further analysis. DESeq2 (<https://github.com/mikelove/DESeq2>) was used to screen for DEGs, followed by `ashr` to remove noise and preserve large differences (32,33). DEGs from bulk RNA-seq were defined using the standard criteria ($\log_2\text{FoldChange} < -1$ or > 1 , adjusted $P < 0.05$). Only genes that were highly expressed in malignant breast tissue ($\log_2\text{FoldChange} > 1$, adjusted $P < 0.05$ in `seqseq`; $\text{avg_log_FC} > 0.25$, adjusted $P < 0.05$ in scRNA-seq) were used to compare the bulk RNA-seq DEGs with those of scRNA-seq. Gene Ontology (GO) enrichment analyses of the different DEGs were performed using the `clusterProfiler` R package (<https://guangchuangyu.github.io/software/clusterProfiler/>), and the function `simplify`

was applied to reduce the redundancy of the enriched GO terms (34). GO terms with adjusted P values less than 0.05 were considered in the final result.

Shiny App construction

We developed an online application, the Gene co-expression Network in Breast Cancer (GCNBC), based on the shiny framework (<https://shiny.rstudio.com/>, with the shinydashboard and shiny R packages), whose workflow was described above. The app was then deployed on the shinyapps.io website (<https://www.shinyapps.io/>). The DT R package was used to present tables, and the igraph package was used to display the figures of the gene co-expression network.

Statistical analysis

The Wilcoxon test was used to analyze the differences between two groups of continuous variables that were non-normally distributed. The chi-square test was used to analyze the variance of categorical variables. The Kaplan-Meier and log-rank tests were used to analyze the survival differences. All data analyses were performed using R version 3.6.3 or Python version 3.8.5. Unless otherwise specified, a P value below 0.05 was considered statistically significant.

Results

Identification of DEGs in malignant epithelial cells

We analyzed the largest breast carcinoma single-cell dataset (GEO: GSE161529) from a public domain, which consisted of 58 samples from *in situ* carcinomas (n=34) and control tissues (including adjacent tissue from breast cancer patients and normal breast tissue from patients without breast cancer, n=24) from 49 patients. We applied a series of strict quality control procedures to remove cells with low-quality data and low-gene expression, and ultimately examined 273,053 cells (166,569 and 106,484 cells for tumor and non-cancerous tissues, respectively). We then annotated and obtained 169,487 epithelial cells according to the expression levels of well-known epithelial cell markers (*KRT* family genes and *CLDN4*), including 104,607 and 64,880 cells for tumor and non-cancerous tissues, respectively (Figure 2A,2B).

We used inferCNV to distinguish non-malignant epithelial cells from tumor samples. The results indicated

that the cell subpopulations from tumor samples were in five clusters (Figure 2C) and that there were large CNVs in all five tumor epithelial cells clusters relative to the normal cells (Figures 2D,2E), which suggested that there were no detectable normal epithelial cells among the tumor samples in these data. We then annotated the epithelial cells as either malignant or non-malignant according to the CNVs, and the results showed there were 104,607 malignant cells and 64,880 non-malignant cells.

Differential expression analysis indicated that there were 1,262 dysregulated genes in the malignant cells relative to the normal cells (adjusted $P < 0.05$, absolute average $\log_{2}FC > 0.25$). Among these, 615 genes exhibited a high expression in malignant cells and 647 genes had high expression in normal cells (Figure 3A, available online: <https://cdn.amegroups.cn/static/public/atm-22-5684-1.xlsx>).

Construction and verification of DEGs in the gene co-expression network

We then examined the possible molecular mechanisms of these 1,262 DEGs by constructing co-expression networks of these DEGs in malignant epithelial cells at a single-cell resolution using Spearman correlation analysis (see our web app GCNBC, <https://prognosticpredictor.shinyapps.io/GCNBC/>, Figure 3B). Among these, we observed a strong correlation in the expressions of *AGR3* and *ESR1* ($\rho = 0.369$, adjusted $P < 0.001$), which is consistent with a previous study that reported this correlation in ER+ breast carcinoma cell lines (35). We also observed that *ADAR*, whose inactivation can lead to a weak IFN response (36), was co-expressed with *IF16* in malignant epithelial cells ($\rho = 0.142$, adjusted $P < 0.001$).

Next, we characterized the signaling pathways in which these DEGs functioned in breast cancer epithelium using functional enrichment analysis for each DEG based on its co-expression network (available online: <https://cdn.amegroups.cn/static/public/atm-22-5684-2.xlsx>). The co-expression networks and functional analyses provided valuable information for studying the function of the dysregulated genes.

We then verified the co-expression networks. We first validated the co-expression of genes in these networks by testing them in more than 300 breast-related transcriptomics data using SEEK (<https://seek.princeton.edu/seek/>), a bioinformatics data portal that analyzes gene co-expression relationships based on the GEO datasets. For this analysis, we selected the three DEGs with the

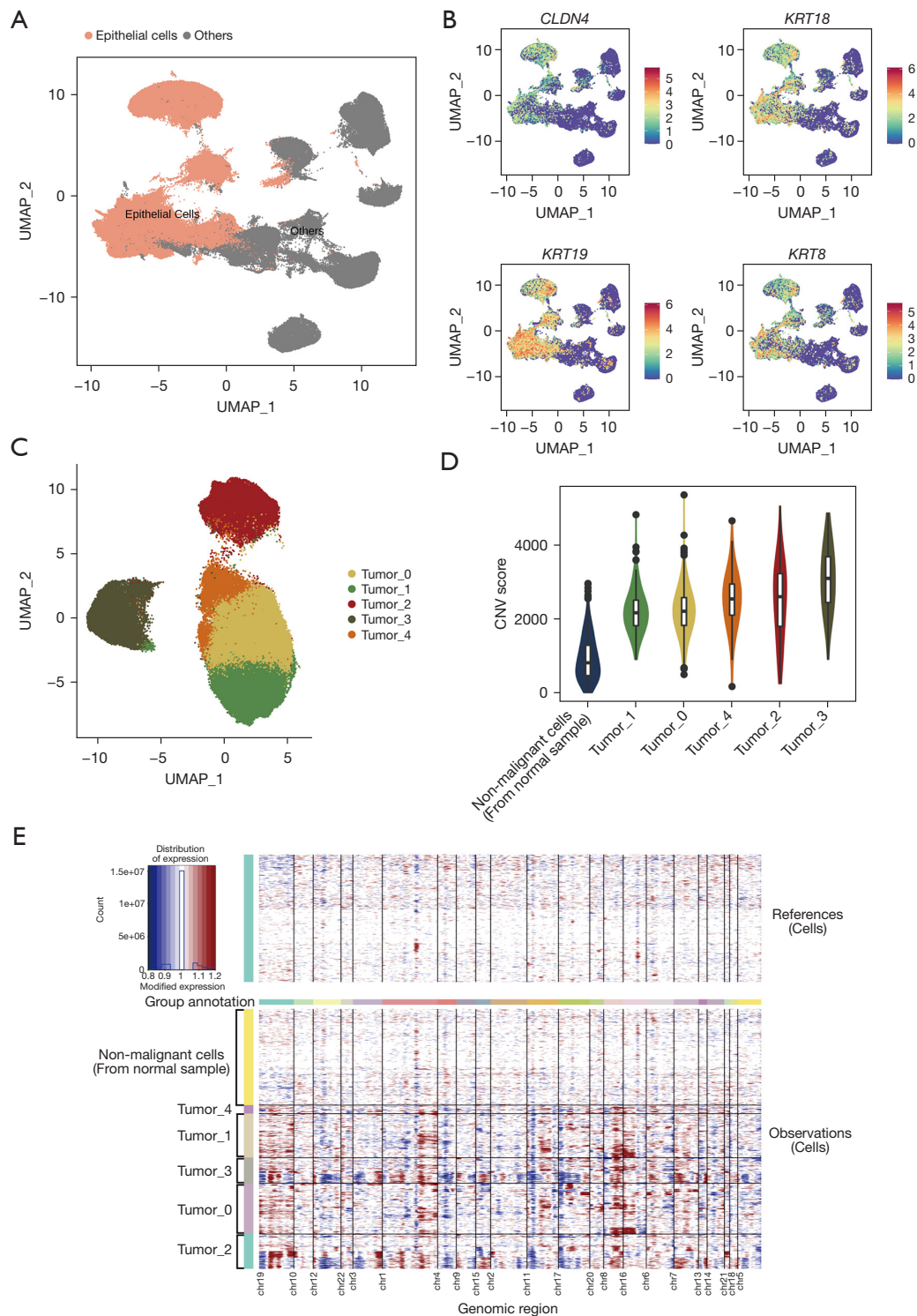


Figure 2 Identification of malignant epithelial cells in breast carcinoma. (A) UMAP plot of 273,053 cells, with classification as epithelial cells or other cell types. (B) Normalized expression of marker genes for epithelial cells (*KRT19*, *KRT8*, *KRT18*, and *CLDN4*). (C) UMAP plot of 104,607 cells from tumor samples grouped into five major clusters based on the Louvain algorithm. (D) Violin plot of all five malignant epithelial cells clusters and cells from non-malignant cells. (E) Heatmap of large-scale CNVs for epithelial cells in five malignant epithelial cell clusters and non-malignant cells (red: gains; blue: losses). CNVs, chromosome copy number variations.

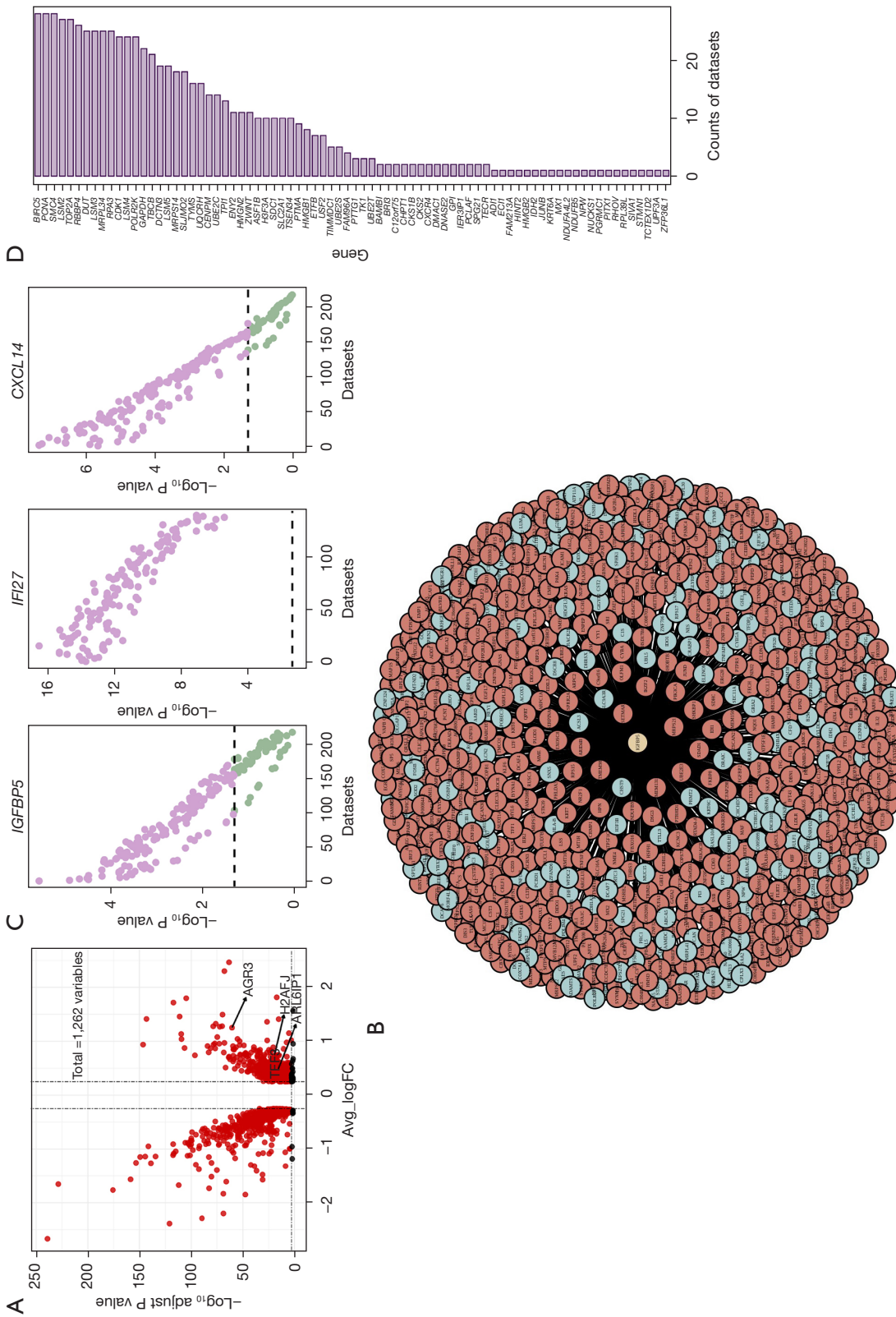


Figure 3 Construction and verification of the DEG co-expression networks. (A) Volcano plot showing the differential expression of malignant epithelial cells based on the scRNA-seq data, including previously reported genes related to breast cancer (*TFF3*, *AGR3*, *H2AF7*, and *ARL6IP1*). Red: Genes meet our screening criteria (see Methods); Black: Genes did not meet our screening criteria (see Methods). (B) Network diagram of the IGFBP5 co-expression network, including previously reported genes (*ASCL1*, *KLF4*, and *OST4*). (C) Dot plots of datasets, which verified the co-expression relationships of target genes (*IGFBP5*: 70.6%, *IFI27*: 100%, *CXCL14*: 72.9%) in the breast-related data. Purple: datasets consistent with our results ($P < 0.05$). Green: datasets inconsistent with our results ($P \geq 0.05$). (D) Bar plot showing the number of CRISPR screen datasets that considered the target genes as being related to cell proliferation. Avg_logFC, log fold-change of the average expression between the malignant epithelial cells and non-malignant epithelial cells; DEG, differentially expressed gene; scRNA-seq, single-cell RNA sequencing.

Table 1 Characteristics of breast carcinoma patients

| Characteristic | TCGA cohort | | | METABRIC cohort (N=1,764) |
|---------------------------|----------------------|------------------|-----------------|---------------------------|
| | Training set (N=584) | Test set (N=389) | Overall (N=973) | |
| Race | | | | |
| White | 447 (76.5) | 291 (74.8) | 738 (75.8) | – |
| Black or African American | 96 (16.4) | 80 (20.6) | 176 (18.1) | – |
| Others | 41 (7.0) | 18 (4.6) | 59 (6.1) | – |
| Age, years | 59 [26, 90] | 55 [27, 90] | 58 [26, 90] | 61 [51, 70] |
| TNM stage | | | | |
| I | 106 (18.2) | 70 (18.0) | 176 (18.1) | 630 (35.7) |
| II | 338 (57.9) | 220 (56.6) | 558 (57.3) | 979 (55.5) |
| III | 131 (22.4) | 92 (23.7) | 223 (22.9) | 144 (8.16) |
| IV | 9 (1.5) | 7 (1.8) | 16 (1.6) | 11 (0.62) |

Data are presented as n (%) or median [25 percentile, 75 percentile]. TCGA, The Cancer Genome Atlas; METABRIC, Molecular Taxonomy of Breast Cancer International Consortium; TNM stage, the tumor, node, metastasis staging system of malignant tumors.

largest average logFC (*IGFBP5*, *IFI27*, and *CXCL14*; available online: <https://cdn.amegroups.com/static/public/atm-22-5684-1.xlsx>) using the top 100 co-expressed genes ranked by RS (due to the input limitations of SEEK). The results indicated co-expression of the tested DEGs and the corresponding 100 genes in most breast cancer-related datasets (70.6% for *IGFBP5*, 100% for *IFI27*, and 72.9% for *CXCL14*; *Figure 3C*), which support the reliability of our co-expression networks.

We then verified the functional annotation of the co-expression networks. Among the 1,262 epithelial genes related to malignancy, we analyzed the association between 163 genes and cell proliferation based on the functional annotation of their co-expression networks (available online: <https://cdn.amegroups.com/static/public/atm-22-5684-3.xlsx>). We validated the association of these 163 genes with cell proliferation using the published CRISPR screening data from BioGRID. CRISPR screening is a large-scale genetic loss-of-function experimental approach that can provide experimental evidence of key genes and identify a specific phenotype in a specific cell line (37). There were 31 CRISPR screening studies related to breast cancer and cell proliferation, and 81 of the 163 genes we analyzed were correlated with proliferation in at least one of the CRISPR screens (*Figure 3D*). These CRISPR screening results provide experimental support for the validity of the functional annotation of our co-expression networks and support the reliability of our functional annotation results.

Prognostic model based on single-cell DEGs

To evaluate the potential use of DEGs for prognostic prediction and risk stratification, we screened the 1,262 DEGs in 973 breast carcinoma patients from TCGA (including 584 in the training set and 389 in the testing set, *Table 1*) using the iterative LASSO technique. Since there was a large decline in frequency between the tenth and eleventh most frequent genes (*Figure S1*), we examined 10 candidate genes (*MAL2*, *BAMBI*, *ALDH3B2*, *TMEM14B*, *MTRNR2L12*, *SDCBP2*, *DAB2*, *TARS*, *CSTA*, and *NDUFB1*) to define the individual risk score using multivariable Cox regression analysis (*Figure 4A*). The results indicated that none of these genes were statistically significant, which is consistent with the PH assumption (*Figure S2A,S2B*). Thus, we defined the risk score using the following equation:

$$\begin{aligned} \text{Risk score} = & 0.0013 \times \text{MAL2} + 0.003 \times \text{BAMBI} + 0.0025 \times \text{ALDH3B2} \\ & - 0.0085 \times \text{TMEM14B} + 0.0241 \times \text{MTRNR2L12} \\ & + 0.0287 \times \text{SDCBP2} + 0.0095 \times \text{DAB2} + 0.0121 \times \text{TRAS} \\ & - 0.0105 \times \text{CSTA} - 0.0008 \times \text{NDUFB1} \end{aligned} \quad [3]$$

We also classified patients into low- or high-risk groups according to the optimal cut-off value for this risk score.

Given that tumor stage, patient age, and risk group were related to prognosis in the univariate Cox analysis (*Table 2*), we examined these three factors in the prognostic model using multivariate Cox analysis. The results showed that risk group was an independent prognostic factor (*Table 2*, *Figure 4B*). In addition, our model performed well in the training and

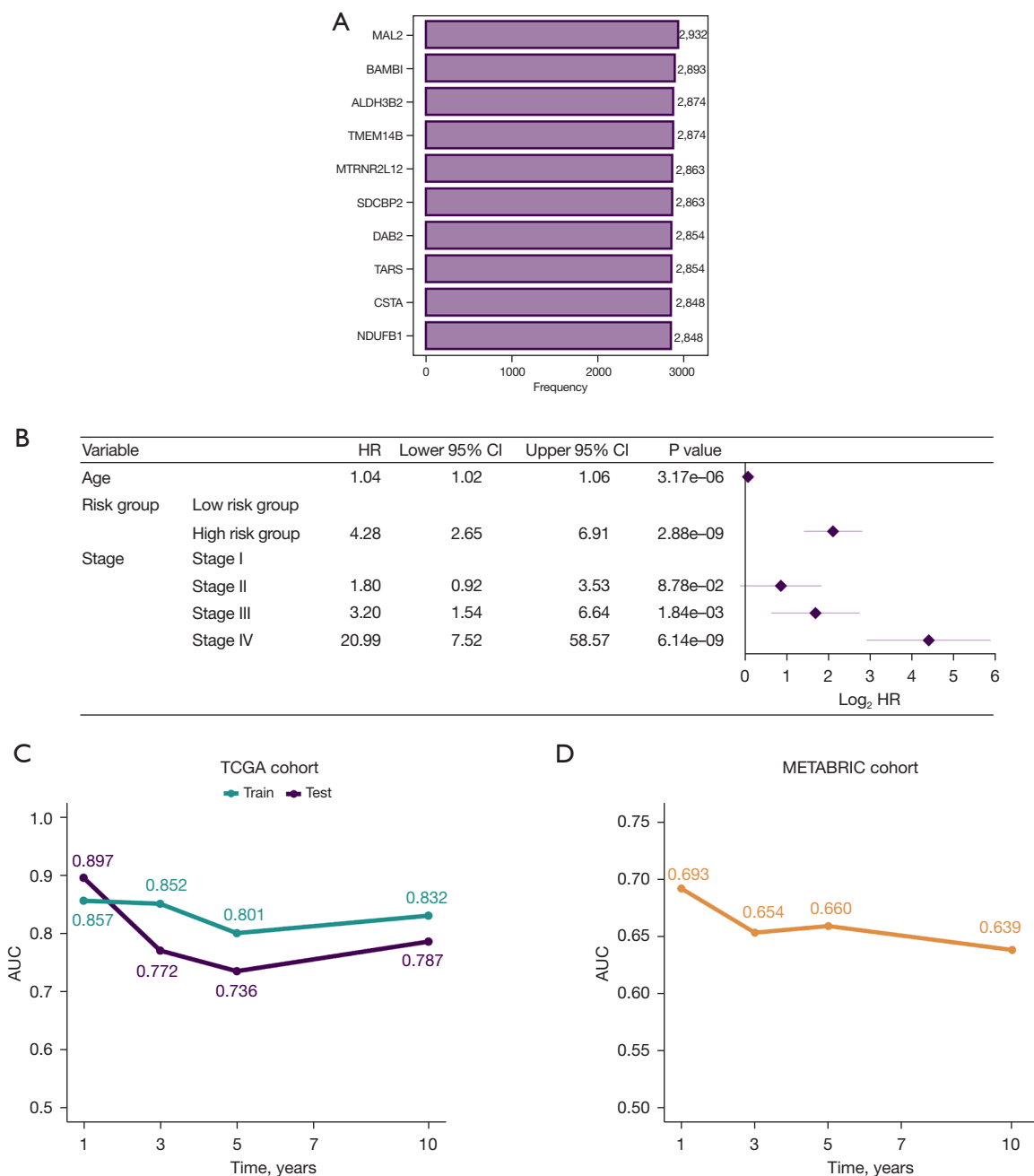


Figure 4 Construction and evaluation of a prognostic model based on single-cell DEGs. (A) Bar plot showing the frequencies of the top 10 genes in the 3,000 iterations from the LASSO-penalized multivariate Cox proportional hazards model. (B) Forest plot of the multivariate Cox regression analysis. (C) Line plot of the time-dependent AUC values in the training and test sets (TCGA cohort). (D) Line plot of the time-dependent AUC values in the external cohort (METABRIC cohort). HR, hazard ratio; CI, confidence interval; AUC, area under curve; DEG, differentially expressed gene; TCGA, The Cancer Genome Atlas.

testing sets at all of the tested follow-up times (Figure 4C, Table 3), with AUC values ranging from 0.801 to 0.857 (training set) and 0.736 to 0.897 (test set). Furthermore,

the model was tested on an external cohort (Table 1). The results showed that our model also performed well in the external cohort, with AUC values ranging from 0.639 to

Table 2 Univariate and multivariate Cox regression analysis of factors associated with overall survival

| Characteristic | Univariate Cox regression | | Multivariate Cox regression | | | |
|---------------------------|---------------------------|--------|-----------------------------|----------------|------|----------------|
| | HR (95% CI) | P | HR (95% CI) | P [#] | VIF | P [*] |
| Age | 1.04 (1.02, 1.06) | <0.001 | 1.04 (1.02, 1.06) | <0.001 | 1.02 | 0.51 |
| Race | | | | | | |
| White | Ref | Ref | – | – | – | – |
| Black or African American | 0.98 (0.54, 1.77) | 0.937 | – | – | – | – |
| Others | 0.71 (0.17, 2.93) | 0.64 | – | – | – | – |
| Risk group | | | | | | |
| Low risk | Ref | Ref | Ref | Ref | 1.01 | 0.53 |
| High risk | 4.06 (2.52, 6.53) | <0.001 | 4.28 (2.65, 6.91) | <0.001 | – | – |
| TNM stage | | | | | | |
| I | Ref | Ref | Ref | Ref | 1.04 | 0.22 |
| II | 1.49 (0.76, 2.9) | 0.245 | 1.8 (0.92, 3.53) | 0.088 | – | – |
| III | 2.45 (1.19, 5.06) | 0.015 | 3.2 (1.54, 6.64) | 0.002 | – | – |
| IV | 14.98 (5.46, 41.12) | <0.001 | 20.99 (7.52, 58.57) | <0.001 | – | – |

[#], P value from multivariate Cox regression. ^{*}, P value from the proportional hazards assumption. HR, hazard ratio; CI, confidence interval; VIF, variance inflation factor; TNM stage, the tumor, node, metastasis staging system of malignant tumors.

Table 3 Time-dependent AUC values in datasets

| Cohort | Timepoint | AUC (95% CI) |
|------------|-----------|----------------------|
| TCGA_Train | 1 | 0.857 (0.744, 0.95) |
| TCGA_Train | 3 | 0.852 (0.788, 0.922) |
| TCGA_Train | 5 | 0.801 (0.736, 0.867) |
| TCGA_Train | 10 | 0.832 (0.739, 0.917) |
| TCGA_Test | 1 | 0.897 (0.811, 0.977) |
| TCGA_Test | 3 | 0.772 (0.688, 0.854) |
| TCGA_Test | 5 | 0.736 (0.664, 0.828) |
| TCGA_Test | 10 | 0.787 (0.634, 0.97) |
| METABRIC | 1 | 0.693 (0.609, 0.812) |
| METABRIC | 3 | 0.654 (0.624, 0.687) |
| METABRIC | 5 | 0.660 (0.632, 0.685) |
| METABRIC | 10 | 0.639 (0.665, 0.665) |

AUC, area under curve; TCGA, The Cancer Genome Atlas; METABRIC, Molecular Taxonomy of Breast Cancer International Consortium; CI, confidence interval.

0.693 (Figure 4D, Table 3).

Comparison of the DEGs from scRNA-seq and bulk RNA-seq

To determine the value of using single-cell analysis, we compared the transcriptional changes of gene expression in breast cancer using scRNA-seq and bulk RNA-seq. The results showed that most of the genes (n=18,194) were detected both in scRNA-seq and bulk RNA-seq data; however, the DEGs in these datasets differed significantly, and there were only 182 common DEGs (Figure 5A). Moreover, 2,599 DEGs that were identified using bulk RNA-seq data were not identified as DEGs in the scRNA-seq data. These genes included some marker genes of cell types other than epithelial cells (available online: <https://cdn.amegroups.com/static/public/atm-22-5684-4.xlsx>), such as *CD3D* (T-cell marker) and *CD19* (B-cell marker). Consistently, the GO results of the 2,599 DEGs suggested their involvement in various non-malignant-cell-related

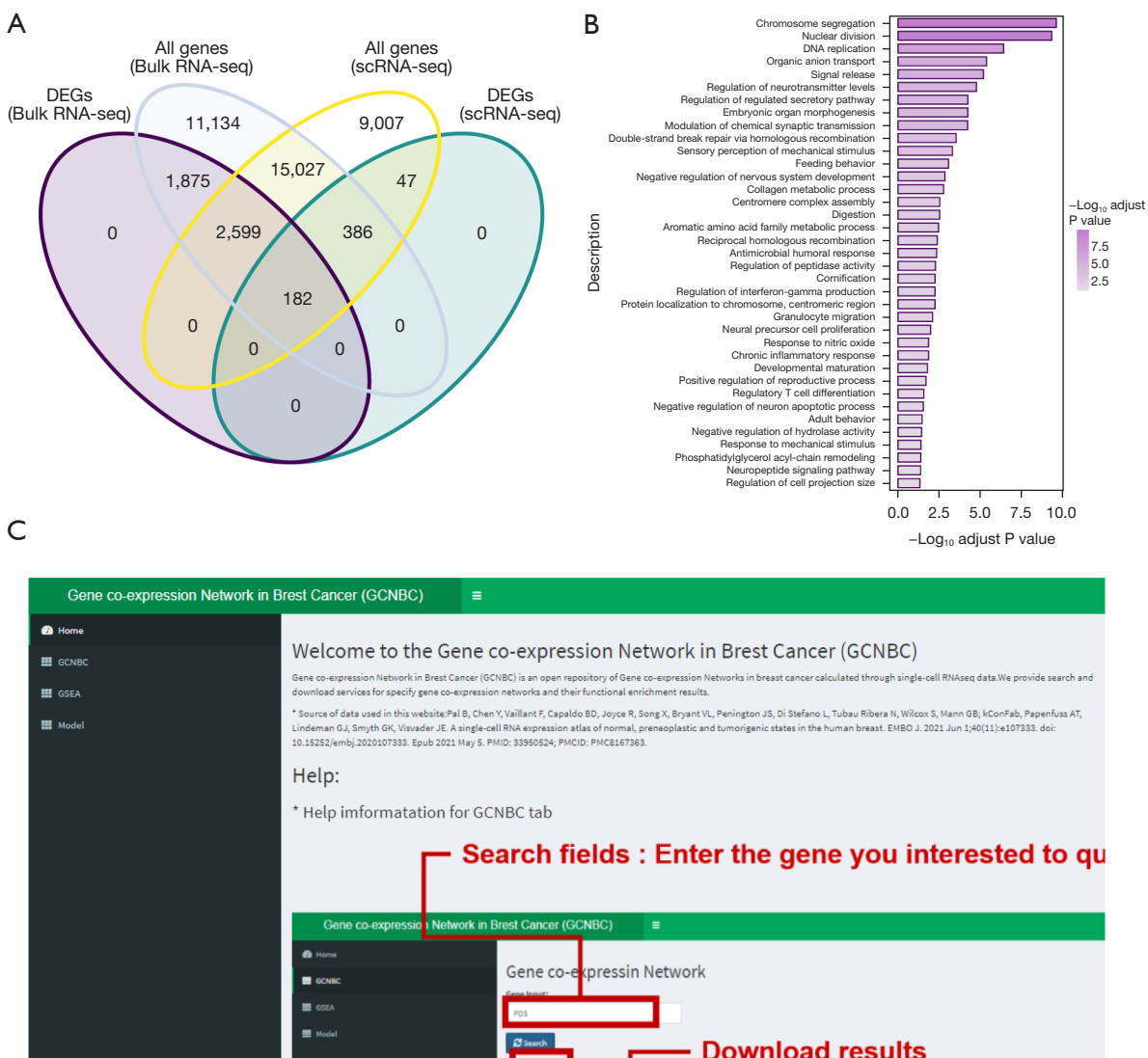


Figure 5 Comparison of DEGs identified by scRNA-seq and bulk RNA-seq. (A) Venn plot of DEGs identified by scRNA-seq and bulk RNA-seq. (B) Bar plot of pathway enrichment results (GO terms) for 2,599 genes that were detected by scRNA-seq and bulk RNA-seq but only identified as DEGs in bulk RNA-seq data. (C) Screenshot of our analytic data portal, the GCNBC. DEG, differentially expressed gene; scRNA-seq, single-cell RNA sequencing; Bulk RNA-seq, bulk RNA-sequencing; GO, Gene Ontology; GCNBC, Gene Co-expression Network in Breast Cancer.

processes, such as regulatory T-cell differentiation and neural precursor cell proliferation (Figure 5B). Thus, we believe that the complex cell composition of bulk carcinoma tissue leads to confounding bias when performing bulk RNA-seq data analysis. In contrast, the DEGs identified using high-quality scRNA-seq data provided more specific and accurate descriptions of DEGs in breast carcinoma epithelial cells.

GCNBC web apps

All of our results are publicly available via an interactive web application (Figure 5C), Gene Co-expression Network in Breast Cancer (GCNBC; <https://prognosticpredictor.shinyapps.io/GCNBC/>). The menu on the left of the web app provides options including “Home” (introduction and tutorial), “GCNBC” (access portal to our gene co-

expression network results), “GSEA” (our GSEA functional enrichment analysis results), and “Model” (our prognostic models). Users can get the predictive results by putting the gene expression and clinical information into the “Model” module in our web app.

Discussion

ScRNA-seq technology is a new method that allows researchers to examine the heterogeneity of cancer cells within a tumor, discover novel potential therapeutic biomarkers, and study the co-expression relationships between genes at single-cell resolutions. We performed a comprehensive analysis of breast carcinoma datasets at the level of single cells by examining 169,487 breast epithelial cells (including 104,607 malignant epithelial cells and 6,484 non-malignant epithelial cells) to characterize the transcriptomic changes of epithelial cells in breast carcinoma. Through this analysis, we identified 1,262 genes that form a signature for breast carcinoma and then described their functions and co-expression networks. Notably, several novel genes that were highly expressed in breast cancer cells—*H2AF7* and *ARL61P1*—have established functions in the resistance to cell proliferation in glioblastoma multiforme (38) and cervical cancer (39). Some of the DEGs identified herein were also highly expressed in breast carcinoma cells, such as *TFF3* (40) and *AGR3* (35,41,42). Previous research suggests that *TFF3* promotes angiogenesis in breast cancer (43), and *AGR3* promotes the proliferation and migration of malignant breast cancer cells and functions in the resistance of breast carcinoma to tamoxifen (35,41,42). These results confirm the robustness of our analytic pipeline and enabled the identification of DEGs that play important roles in the development of breast carcinoma. Moreover, our comparison of DEGs from the scRNA-seq and bulk RNA-seq data demonstrated the advantages of studying transcriptomic changes using scRNA-seq data.

Although single-cell sequencing technology can detect tumor-related genes and characterize their co-expression networks, most current scRNA-seq research of breast carcinoma focuses on the tumor immune microenvironment or the detection of heterogeneous clusters among tumor cells. Large-scale single-cell data can elucidate malignancy-related genes in breast cancer and their co-expression networks well. Our study is the first to present the co-expression networks of 1,262 DEGs in breast carcinoma epithelial cells at a single-cell resolution.

We then performed a functional annotation analysis of these networks to annotate the function of the dysregulated genes. Although we did not experimentally validate these co-expression networks or their functional annotations, a secondary analysis of the data from public co-expression datasets (SEEK) and public CRISPR screens showed consistent results. Our findings provide an important foundation and insights for subsequent research. Finally, we provided a user-friendly web application so that other researchers can access our results, including the co-expression networks and functional annotation results. The findings presented here improve our understanding of the mechanisms of breast carcinoma at the level of individual cells and provide new insights for the development of targeted therapies.

Numerous studies have constructed prognostic models for cancer based on scRNA-seq and bulk RNA-seq datasets in other tumors; however, none have been developed for breast cancer (14-16,43). Using the iterative LASSO method, we identified 10 genes that had good prognostic value and could be used to reliably stratify different populations (44). We then utilized these results to develop a prognostic model for breast cancer, expressed as a risk score. Our model not only performed well in both the internal and external cohorts, which indicated that it has tremendous prognostic ability. This reflects the ability of our gene set to be used for patient stratification and prognostic prediction. Previous studies reported that six of the 10 genes included in our risk model play roles in breast tumor promotion or suppression: *CALML5*, *BAMBI*, *QPRT*, *CLDN7*, *TARS*, and *NDUFB1* (44-49). Three of the 10 genes (*NDUFB10*, *SERPINA3*, and *PHLDB2I*) were not previously identified as related to breast cancer but were reportedly related to other cancers (50-52). Furthermore, one of the 10 genes (*MAL2*) was reported to mediate the endocytosis and degradation of MHC-I complexes, which could lead to immune evasion of breast cancer cells (53). Our gene co-expression networks showed that the functions of these genes might be broader than previously thought. For instance, we found that *BAMBI* was related to tumor growth and oxidative phosphorylation (available online: <https://cdn.amegroups.cn/static/public/atm-22-5684-2.xlsx>). More work is needed to examine the underlying mechanisms of these 10 genes in breast carcinoma. However, despite our model's strengths, there are still limitations. For instance, we did not analyze patients with missing information, and this model should be validated using a greater number of samples.

Conclusions

In this study, we performed a comprehensive analysis of breast carcinoma using single-cell gene transcription data. We identified a set of potential genes that contribute to breast carcinoma tumorigenesis and tumor development and can be used for prognostic prediction. We also annotated these genes and constructed co-expression networks based on the single-cell data of malignant epithelial cells. Finally, we built a well-performing prognostic model of breast cancer based on scRNA-seq and bulk RNA-seq, which can also be used for prognostic prediction. Taken together, our results provide insights into the mechanisms underlying breast carcinoma progression and suggest potential therapeutic strategies for the treatment of this cancer.

Acknowledgments

Funding: This work was supported by the Basic and Applied Basic Research Fund of Guangdong Province (No. 2022A1515012387).

Footnote

Reporting Checklist: The authors have completed the TRIPOD reporting checklist. Available at <https://atm.amegroupp.com/article/view/10.21037/atm-22-5684/rc>

Conflicts of Interest: All authors have completed the ICMJE uniform disclosure form (available at <https://atm.amegroupp.com/article/view/10.21037/atm-22-5684/coif>). The authors have no conflicts of interest to declare.

Ethical Statement: The authors are accountable for all aspects of the work in ensuring that questions related to the accuracy or integrity of any part of the work are appropriately investigated and resolved. The study was conducted in accordance with the Declaration of Helsinki (as revised in 2013).

Open Access Statement: This is an Open Access article distributed in accordance with the Creative Commons Attribution-NonCommercial-NoDerivs 4.0 International License (CC BY-NC-ND 4.0), which permits the non-commercial replication and distribution of the article with the strict proviso that no changes or edits are made and the original work is properly cited (including links to both the formal publication through the relevant DOI and the license). See: <https://creativecommons.org/licenses/by-nc-nd/4.0/>.

References

1. Sung H, Ferlay J, Siegel RL, et al. Global Cancer Statistics 2020: GLOBOCAN Estimates of Incidence and Mortality Worldwide for 36 Cancers in 185 Countries. *CA Cancer J Clin* 2021;71:209-49.
2. Harbeck N, Penault-Llorca F, Cortes J, et al. Breast cancer. *Nat Rev Dis Primers* 2019;5:66.
3. Ma RM, Yang F, Huang DP, et al. The Prognostic Value of the Expression of SMC4 mRNA in Breast Cancer. *Dis Markers* 2019;2019:2183057.
4. Kariri Y, Toss MS, Alsaleem M, et al. Ubiquitin-conjugating enzyme 2C (UBE2C) is a poor prognostic biomarker in invasive breast cancer. *Breast Cancer Res Treat* 2022;192:529-39.
5. Peng Y, Li H, Fu Y, et al. JAM2 predicts a good prognosis and inhibits invasion and migration by suppressing EMT pathway in breast cancer. *Int Immunopharmacol* 2022;103:108430.
6. Chung W, Eum HH, Lee HO, et al. Single-cell RNA-seq enables comprehensive tumour and immune cell profiling in primary breast cancer. *Nat Commun* 2017;8:15081.
7. Wu SZ, Roden DL, Wang C, et al. Stromal cell diversity associated with immune evasion in human triple-negative breast cancer. *EMBO J* 2020;39:e104063.
8. Azizi E, Carr AJ, Plitas G, et al. Single-Cell Map of Diverse Immune Phenotypes in the Breast Tumor Microenvironment. *Cell* 2018;174:1293-308.e36.
9. Li X, Wang C-Y. From bulk, single-cell to spatial RNA sequencing. *International Journal of Oral Science* 2021;13:36.
10. Klein AM, Mazutis L, Akartuna I, et al. Droplet barcoding for single-cell transcriptomics applied to embryonic stem cells. *Cell* 2015;161:1187-201.
11. Macosko EZ, Basu A, Satija R, et al. Highly Parallel Genome-wide Expression Profiling of Individual Cells Using Nanoliter Droplets. *Cell* 2015;161:1202-14.
12. Trapnell C. Defining cell types and states with single-cell genomics. *Genome Res* 2015;25:1491-8.
13. Chen W, Morabito SJ, Kessenbrock K, et al. Single-cell landscape in mammary epithelium reveals bipotent-like cells associated with breast cancer risk and outcome. *Commun Biol* 2019;2:306.
14. Chen K, Liu X, Liu W, et al. Development and validation of prognostic and diagnostic model for pancreatic ductal adenocarcinoma based on scRNA-seq and bulk-seq datasets. *Hum Mol Genet* 2022;31:1705-19.
15. Zheng P, Zhang H, Jiang W, et al. Establishment of a Prognostic Model of Lung Adenocarcinoma Based on

- Tumor Heterogeneity. *Front Mol Biosci* 2022;9:807497.
16. Chen Z, Wang Y, Li D, et al. Single-Cell RNA Sequencing Revealed a 3-Gene Panel Predicted the Diagnosis and Prognosis of Thyroid Papillary Carcinoma and Associated With Tumor Immune Microenvironment. *Front Oncol* 2022;12:862313.
 17. Pal B, Chen Y, Vaillant F, et al. A single-cell RNA expression atlas of normal, preneoplastic and tumorigenic states in the human breast. *EMBO J* 2021;40:e107333.
 18. Wolock SL, Lopez R, Klein AM. Scrublet: Computational Identification of Cell Doublets in Single-Cell Transcriptomic Data. *Cell Syst* 2019;8:281-91.e9.
 19. Young MD, Behjati S. SoupX removes ambient RNA contamination from droplet-based single-cell RNA sequencing data. *Gigascience* 2020;9:giaa151.
 20. Stuart T, Butler A, Hoffman P, et al. Comprehensive Integration of Single-Cell Data. *Cell* 2019;177:1888-1902.e21.
 21. Korsunsky I, Millard N, Fan J, et al. Fast, sensitive and accurate integration of single-cell data with Harmony. *Nat Methods* 2019;16:1289-96.
 22. Li Y, Jiang T, Zhou W, et al. Pan-cancer characterization of immune-related lncRNAs identifies potential oncogenic biomarkers. *Nat Commun* 2020;11:1000.
 23. Korotkevich G, Sukhov V, Budin N, et al. Fast gene set enrichment analysis. 2021:060012.
 24. Subramanian A, Tamayo P, Mootha VK, et al. Gene set enrichment analysis: a knowledge-based approach for interpreting genome-wide expression profiles. *Proc Natl Acad Sci U S A* 2005;102:15545-50.
 25. Zhu Q, Wong AK, Krishnan A, et al. Targeted exploration and analysis of large cross-platform human transcriptomic compendia. *Nat Methods* 2015;12:211-4, 3 p following 214.
 26. Oughtred R, Rust J, Chang C, et al. The BioGRID database: A comprehensive biomedical resource of curated protein, genetic, and chemical interactions. *Protein Sci* 2021;30:187-200.
 27. Liberzon A, Birger C, Thorvaldsdóttir H, et al. The Molecular Signatures Database (MSigDB) hallmark gene set collection. *Cell Syst* 2015;1:417-25.
 28. Goldman MJ, Craft B, Hastie M, et al. Visualizing and interpreting cancer genomics data via the Xena platform. *Nat Biotechnol* 2020;38:675-8.
 29. Sveen A, Ågesen TH, Nesbakken A, et al. ColoGuidePro: a prognostic 7-gene expression signature for stage III colorectal cancer patients. *Clin Cancer Res* 2012;18:6001-10.
 30. Belsley DA. A Guide to using the collinearity diagnostics. *Computer Science in Economics and Management* 1991;4:33-50.
 31. Grambsch PM, Therneau TMJB. Proportional hazards tests and diagnostics based on weighted residuals. 1994;81:515-26.
 32. Love MI, Huber W, Anders S. Moderated estimation of fold change and dispersion for RNA-seq data with DESeq2. *Genome Biol* 2014;15:550.
 33. Stephens M. False discovery rates: a new deal. *Biostatistics* 2017;18:275-94.
 34. Wu T, Hu E, Xu S, et al. clusterProfiler 4.0: A universal enrichment tool for interpreting omics data. *Innovation (Camb)* 2021;2:100141.
 35. Obacz J, Sommerova L, Sicari D, et al. Extracellular AGR3 regulates breast cancer cells migration via Src signaling. *Oncol Lett* 2019;18:4449-56.
 36. Herzner AM, Khan Z, Van Nostrand EL, et al. ADAR and hnRNPC deficiency synergize in activating endogenous dsRNA-induced type I IFN responses. *J Exp Med* 2021;218:e20201833.
 37. Shalem O, Sanjana NE, Hartenian E, et al. Genome-scale CRISPR-Cas9 knockout screening in human cells. *Science* 2014;343:84-7.
 38. Yao J, Weremowicz S, Feng B, et al. Combined cDNA array comparative genomic hybridization and serial analysis of gene expression analysis of breast tumor progression. *Cancer Res* 2006;66:4065-78.
 39. Guo F, Liu Y, Li Y, et al. Inhibition of ADP-ribosylation factor-like 6 interacting protein 1 suppresses proliferation and reduces tumor cell invasion in CaSki human cervical cancer cells. *Mol Biol Rep* 2010;37:3819-25.
 40. Lau WH, Pandey V, Kong X, et al. Trefoil Factor-3 (TFF3) Stimulates De Novo Angiogenesis in Mammary Carcinoma both Directly and Indirectly via IL-8/CXCR2. *PLoS One* 2015;10:e0141947.
 41. Jiang R, Sun Y, Chen X, et al. Estrogen-regulated AGR3 activates the estrogen receptor signaling pathway to promote tamoxifen resistance in breast cancer. *Breast Cancer Res Treat* 2021;190:203-11.
 42. Xu Q, Shao Y, Zhang J, et al. Anterior Gradient 3 Promotes Breast Cancer Development and Chemotherapy Response. *Cancer Res Treat* 2020;52:218-45.
 43. Jiang A, Wang J, Liu N, et al. Integration of Single-Cell RNA Sequencing and Bulk RNA Sequencing Data to Establish and Validate a Prognostic Model for Patients With Lung Adenocarcinoma. *Front Genet* 2022;13:833797.

44. Debold M, Schildberg FA, Linke A, et al. Specific expression of k63-linked ubiquitination of calmodulin-like protein 5 in breast cancer of premenopausal patients. *J Cancer Res Clin Oncol* 2013;139:2125-32.
45. Fusella F, Secli L, Busso E, et al. The IKK/NF- κ B signaling pathway requires Morgana to drive breast cancer metastasis. *Nat Commun* 2017;8:1636.
46. Ósz Á, Lánckzy A, Gyórfy B. Survival analysis in breast cancer using proteomic data from four independent datasets. *Sci Rep* 2021;11:16787.
47. Yue Z, Shusheng J, Hongtao S, et al. Silencing DSCAM-AS1 suppresses the growth and invasion of ER-positive breast cancer cells by downregulating both DCTPP1 and QPRT. *Aging (Albany NY)* 2020;12:14754-74.
48. Zhou Z, Sun B, Huang S, et al. Roles of aminoacyl-tRNA synthetase-interacting multi-functional proteins in physiology and cancer. *Cell Death Dis* 2020;11:579.
49. Zhang Y, Tian J, Qu C, et al. Overexpression of SERPINA3 promotes tumor invasion and migration, epithelial-mesenchymal-transition in triple-negative breast cancer cells. *Breast Cancer* 2021;28:859-73.
50. Ellinger J, Poss M, Brüggemann M, et al. Systematic Expression Analysis of Mitochondrial Complex I Identifies NDUFS1 as a Biomarker in Clear-Cell Renal-Cell Carcinoma. *Clin Genitourin Cancer* 2017;15:e551-62.
51. Shangguan L, Ti X, Krause U, et al. Inhibition of TGF- β /Smad signaling by BAMBI blocks differentiation of human mesenchymal stem cells to carcinoma-associated fibroblasts and abolishes their protumor effects. *Stem Cells* 2012;30:2810-9.
52. Zeng Z, Cheng J, Ye Q, et al. A 14-Methylation-Driven Differentially Expressed RNA as a Signature for Overall Survival Prediction in Patients with Uterine Corpus Endometrial Carcinoma. *DNA Cell Biol* 2020;39:975-91.
53. Dersh D, Yewdell JW. Immune MAL2-practice: breast cancer immunoevasion via MHC class I degradation. *J Clin Invest* 2021;131:144344.

(English Language Editor: A. Kassem)

Cite this article as: Ruan Z, Chi D, Wang Q, Jiang J, Quan Q, Bei J, Peng R. Development and validation of a prognostic model and gene co-expression networks for breast carcinoma based on scRNA-seq and bulk-seq data. *Ann Transl Med* 2022;10(24):1333. doi: 10.21037/atm-22-5684